

Fatigue Crack Growth Rate in Long Term Operated 19th Century Puddle Iron

Grzegorz Lesiuk^{1, a *}, Jose A.F.O. Correia^{2, b}, Michał Smolnicki^{1, c},
Abilio M.P. De Jesus^{2, d}, Monika Duda^{1, e}, Pedro Montenegro^{2, f},
Rui A.B. Calcada^{2, g}

¹ Wrocław University of Science and Technology, Faculty of Mechanical Engineering,
Department of Mechanics, Materials Science and Engineering, Smoluchowskiego 25, 50-370
Wrocław, +48 71 3203919, POLAND

²Faculty of Engineering, University of Porto, Rua Dr. Roberto Frias, 4200-465 Porto, (+351)
966559442, Portugal

^agrzegorz.lesiuk@pwr.edu.pl, ^bjacorreia@fe.up.pt, ^cmichal.smolnicki@pwr.edu.pl,
^dajesus@fe.up.pt, ^emonika.duda@pwr.edu.pl, ^fpires@fe.up.pt, ^gruiabc@fe.up.pt

Keywords: Puddle Iron, Fatigue Crack Growth, Crack Closure, Strain Energy Parameter

Abstract. The paper presents the results of an experimental investigation of the fatigue crack growth in plane specimens made from puddle iron. Eiffel Bridge from Portugal and 19th-century viaduct steel member from Poland. The tests were performed under the load ratios $R = 0.05, 0.1$ and 0.5 . There were also considered the different description of fatigue crack growth rate using strain energy density parameter based on cyclic J -integral. The fatigue crack growth rate in the tested material is significantly higher than its “ancient” equivalent i.e. old 19th-century mild steel. There is also a noticeable strong contribution of the crack closure effect.

Introduction

It is essential to study the structural integrity of old metallic bridges in order to understand their limitations regarding both material and structure [1]. One aspect to consider is the fatigue behaviour of riveted structural details and materials. The metal bridges of the late 19th and early 20th centuries were built with metallic materials, nowadays called puddled steel or iron [1,2]. These properties are essential for residual life analysis of metallic bridges in order to extend the lifetime of these structures. The metallic material under study was obtained from beam elements extracted from the Eiffel riveted metallic bridge, designed by Gustave Eiffel and inaugurated on June 30, 1878. This bridge is located in Viana do Castelo, Portugal, crossing the Lima River, having a total length of 645 m. Another part of an ancient iron member was extracted from the restored viaduct (1863) located in Brochocin (Low Silesia, Poland). Due to limited knowledge of the fatigue crack growth behaviour [3], this paper fills the gap in the literature on experimental results of fatigue crack growth (FCG) behaviour based on the effective stress intensity factor range and of a new parameter using the strain energy density concept for the metallic materials under consideration [4]. These FCG results are of great importance, since it allows the residual lifetime assessment of old metallic bridges of the same historical period, reducing the uncertainties associated with this type of materials.

Material Investigation

This work is focused on the chemical analysis (C, Mn, Si, P, S) of the tested ancient material using spectra method (measurement station presented in Table 1 results represent the mean value of three measurements) and the microstructural analysis in the post-operated state. The

metallographic inspection was performed at magnification range from 100× to 1000× on non-etched and etched state of the sample (5% HNO₃) using the metallographic microscope following the ASTM E407 - 07(2015)e1 [5]. Images were registered by coupled with microscope digital camera CMOS 15MPx with the software for image analysis.

Table 1. The chemical composition of tested materials (in % by weight)

Investigated materials	C	Mn	Si	P	S
Eiffel Bridge	<0.01	0.01	0.07	0.354	0.045
Puddle iron 1863 [2]	0.08	0.025	0.15	0.245	0.015

Based only on the chemical analysis there is noticeable high phosphorus content in both materials. This fact indicates for possible classification of the tested materials as a puddle iron. Based on the theory of degradation of old puddle iron [6,7], the low carbon content (<0.1% C) and lack of the de-oxidation element – Si predestine this material for the microstructural degradation processes.

The microstructure of the tested materials is presented in Figs. 1-4. The static tensile results are collected in Table 2.

Table 2. Static tensile test results

Material	f_y [MPa]	f_u [MPa]	E [GPa]	A_5 [%]	Z [%]
Eiffel Bridge	292	342	193	8.1	11.6
Puddle iron 1863 [2]	287	360	191	15.3	33.9

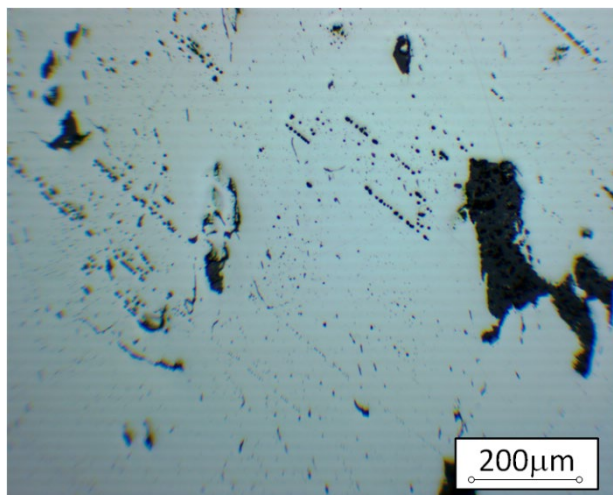


Fig. 1. Representative image of the material (Eiffel Bridge) structure in the non-etched state. Noticeable large non-metallic inclusions and slags, the size of the slags often exceeds mm, non-etched state [8].

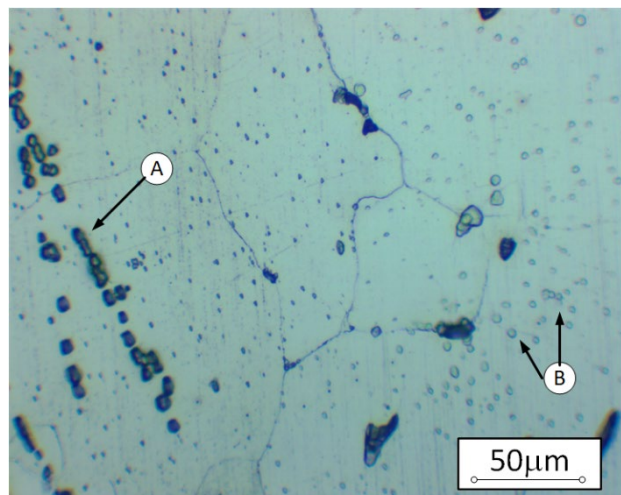


Fig. 2. Enlarged ferrite grains with non-metallic inclusion chains (A). Noticeable different grain size with brittle phase precipitations inside ferrite grains (B). Eiffel Bridge, etched 5% HNO₃ [8].

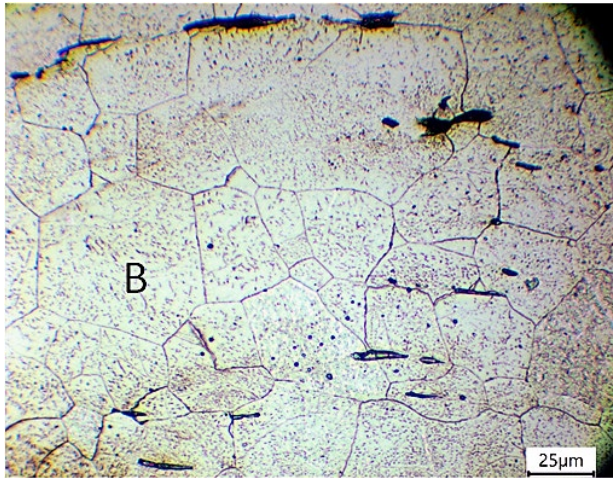


Fig. 3. Enlarged ferrite grains (1863 iron) with non-metallic inclusion chains and degradation precipitations (B), etched 5% HNO₃ [6].

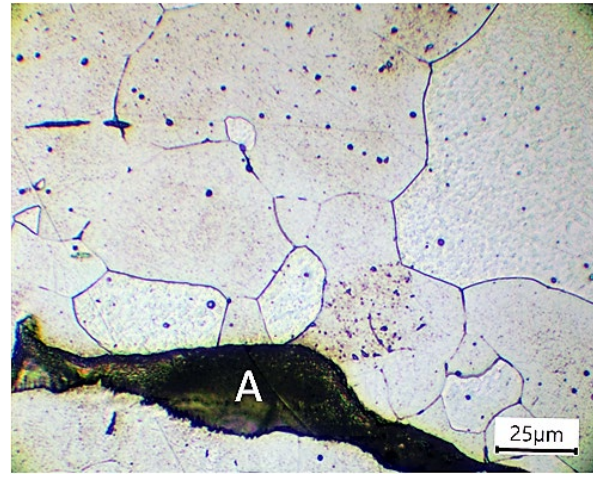


Fig. 4. Magnified ferrite grains with large non-metallic inclusions (A) in iron from viaduct (1863), etched 5% HNO₃ [6].

The microstructure of the investigated materials is shaped by numerous non-metallic inclusions (mainly silicates) and consist of ferrite grains of different size. The presence of the microstructural degradation processes is also confirmed by brittle phase precipitations occurring inside ferrite grains as well as on the grain boundaries. The microstructure of the tested material confirms the fact that the delivered for investigation material is an old puddle iron from the 19th-century – similar like in the previous research findings associated with old steel reported in [7].

Fatigue crack growth rate

In order to predict the remaining fatigue crack growth lifetime, it is essential to know the kinetics of fatigue crack growth. For this purpose, the fatigue crack growth rate was investigated. The used tensile machine, apparatus (e.g. clevises, grips etc.) and specimens (Fig. 5) were same as described in ASTM E647 [9]. The graphs of fatigue crack growth kinematic are presented in coordinates $\log(da/dN) - \log \Delta K (K_{max})$, where, in logarithmic scale, the value of da/dN for specified crack length is marked on the ordinate and $\Delta K, K_{max}$ on the abscissa. The SIF for the CT specimen is specified using formula presented in ASTM E647 [9]:

$$K = \frac{\Delta F}{B\sqrt{W}} f\left(\frac{a}{W}\right), \quad (1)$$

$$f\left(\frac{a}{W}\right) = \frac{(2 + a/W)(0.886 + 4.64a/W - 13.32(a/W)^2 + 14.72(a/W)^3 - 5.6(a/W)^4)}{\sqrt{(1 - a/W)^3}} \quad (2)$$

where: a - crack length; B - specimen thickness; W - specimen width; ΔF - force amplitude.

During the examination were registered the following signals: force, displacements, crack opening displacement (COD). Amid applying of monotonically arising loading, the crack length size was determined by compliance procedures. The function of plane stress elastic compliance for CT specimens is described by the formula [9]:

$$\frac{a}{W} = C_0 + C_1 u_x + C_2 u_x^2 + C_3 u_x^3 + C_4 u_x^4 + C_5 u_x^5. \quad (3)$$

Coefficients $C_0, C_1, C_2, C_3, C_4, C_5$ are fully described by ASTM E647 [9] depending on measurement localisation of COD (Crack Opening Displacement). The u_x quantity is defined as:

$$u_x = \frac{1}{\sqrt{\frac{BEv}{F} + 1}} \quad (4)$$

where: B - specimen thickness; E - elastic modulus; v - COD; F - applied force; v/F - displacement versus force curve slope measured during the test.

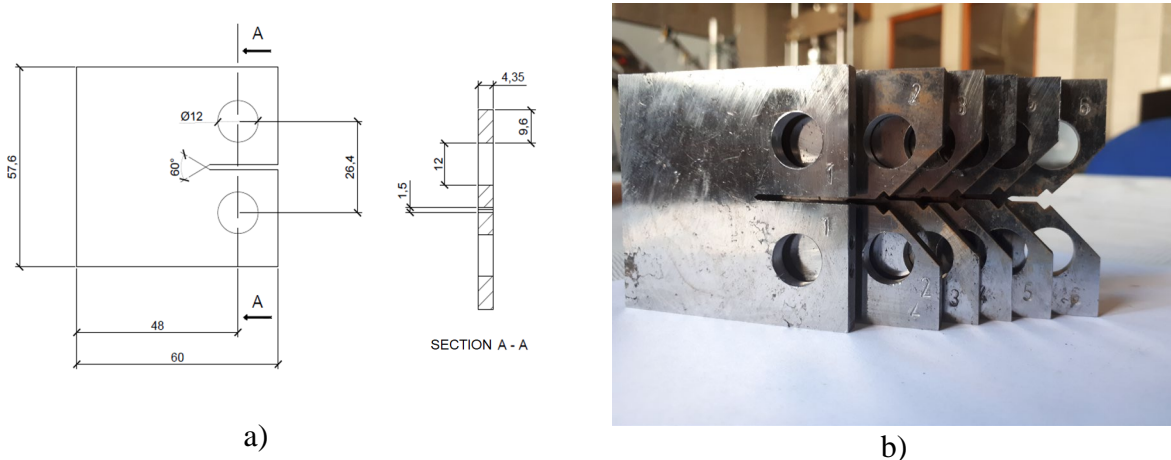
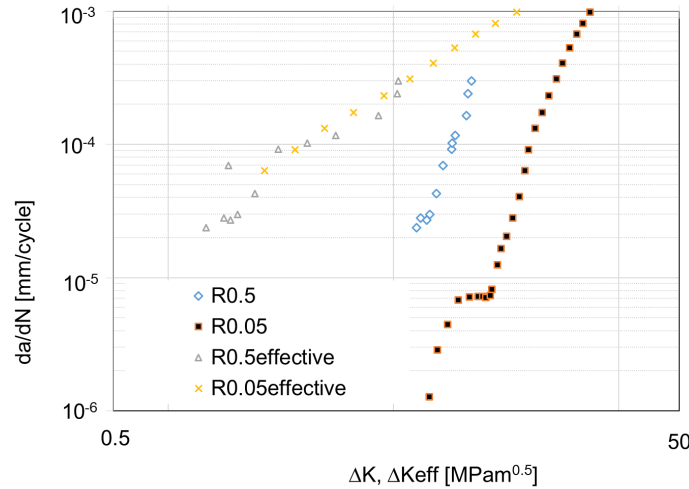


Fig. 5. a) CT specimen for mode I test (Eiffel Bridge) [8], b) machined CT specimens before test

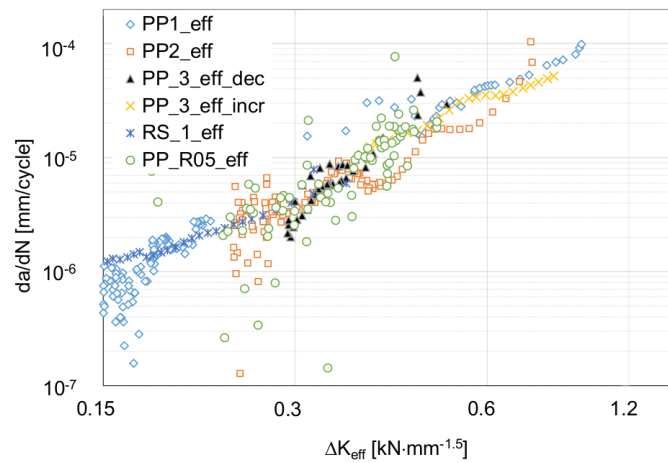
Before the proper investigation, the fatigue pre-crack (mode I) was made preserving all condition of loading described in ASTM E647 [9]. During precracking the ΔK does not exceed 13-15 MPam^{0.5} range. The main test started from the initial value of ΔK in order to avoid the plastic zone influence from the precracking procedure. Experiments were performed for two different mean stress levels characterised by the stress ratio $R = 0.05$ and $R = 0.5$ (for Eiffel Bridge) with sinusoidal loading waveform (frequency $f=5$ Hz). The crack length size was monitored using the phenomenon of plane stress elastic compliance (Eq. 3). The computer system was controlled by MTS FlexTest console and FCGR (Fatigue Crack Growth Rate) software integrated with MTS machine. Periodically, the crack length was controlled and adjusted using a stereoscopic microscope with a digital camera coupled with the tensile machine MTS 810. For the puddle iron from viaduct (1863) similar procedure (fully described in refs. [6,8]) was adopted. Due to material limitations, the size of the CT specimen was decreased. In order to evaluate the fatigue crack growth resistance for such material, tests were performed using two types of Compact Tension (CT) specimens with the main dimensions: $W=38$ mm, $t=6$ mm (thickness). The area of interest was the near-threshold region, of the FCGR curve and stable Paris regime using ΔK -control decreasing/increasing test ($R=0.1, f=12$ Hz). Similarly as in the case of the Eiffel Bridge steel, a signal of the force, COD and displacement were registered.

During the experiment for chosen cycles at least two hysteresis loops were registered in order to assess the F-COD behaviour during test. According to the experimental procedure described in refs. [6,8], the crack closure point as well as corresponded F_{cl} and K_{cl} levels was estimated in order to evaluate the effective stress intensity range (ΔK_{eff}) based on the Elber concept [10].

Finally, the Kinetic Fatigue Fracture Diagrams were constructed for both materials – Fig. 6.



a)



b)

Fig. 6. Kinetic Fatigue Fracture Diagram for; a) Eiffel Bridge, b) puddle iron from viaduct (1863) [6].

A noticeable is R-ratio effect in KFFD represented by shifted da/dN curves (Fig. 6a) for $R=0.5$ and $R=0.05$. In case of the ΔK_{eff} , the effect can be neglected in Paris regime. The same effect is observed for all R-ratios (0.05, 0.1 and 0.5) in fatigue crack growth results for puddle iron from viaduct. In the case of historic steel, the unification of the KFFD notation seems to be a key issue. One of the promising approaches is the energy approach proposed in refs. [11,12]. In the range of linear fracture mechanics a similar effect (R-ratio avoidance) was achieved as for effective ΔK using ΔS^* [11]. It is worth noting that during a cyclic load, J_{max} and ΔJ are the values that bind the local stress intensity in front of the crack front - J plays the same role as K in the elastic-plastic fracture mechanics. Therefore, in the proposed new crack driving force [11] is described as follows:

$$\Delta S^* = \sqrt{\Delta J^+ \cdot J_{max}} \tag{5}$$

For energy fatigue crack growth description (puddle iron from Eiffel bridge) only elastic part of ΔJ -integral range was analysed using well-known relationship from linear-elastic fracture mechanics (with assumed plane stress conditions):

$$\Delta J_e = \frac{\Delta K^2}{E}. \tag{6}$$

The new energy-based kinetic fatigue fracture diagrams are presented in Fig. 7a (based only on cyclic J -integral parameter) and Fig. 7b (based on new ΔS^* parameter). As it is noticeable the new ΔS^* strain energy parameter describes kinetics of fatigue crack growth synonymously and independently from R -ratio.

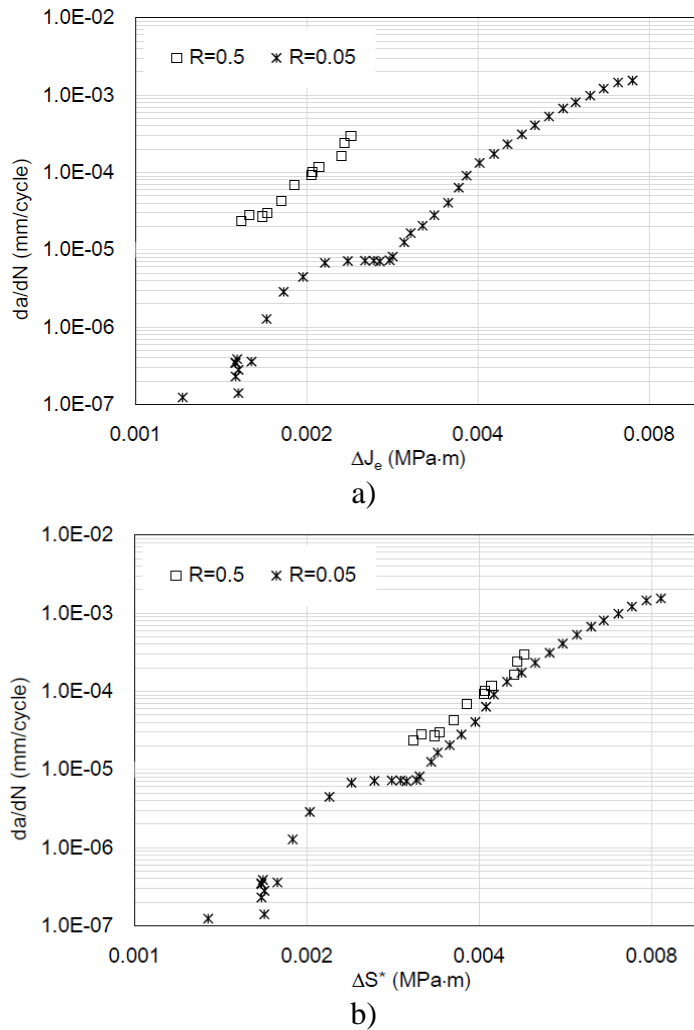


Fig. 7. Kinetic Fatigue Fracture Diagram (KFFD) for Eiffel Bridge steel based on; a) elastic ΔJ_e parameter, b) ΔS^* strain energy density parameter.

Conclusions

Based on the performed experimental tests, some conclusions can be formulated. The Paris' exponent m for old puddle iron seems to be significantly higher than for modern bridge constructional steel. The shifting of the $da/dN-\Delta K_{applied}$ curves was observed for different R -

ratios. Furthermore, the observed fatigue crack closure phenomenon strongly influence the kinetics of fatigue crack growth (via decrease Paris' m exponent and consolidate data from different R -ratios into one curve). The proposed, new energy parameter ΔS^* describes the kinetics of fatigue crack growth in puddle iron effectively without mean stress effect (R -ratio).

References

- [1] G. Lesiuk, B. Rymasa, J. Rabięga, J.A.F.O. Correia, A.M.P. De Jesus, R. Calçada. Influence of loading direction on the static and fatigue fracture properties of the long term operated metallic materials. *Eng Fail Anal* 2019;96:409-425. <https://doi.org/10.1016/j.engfailanal.2018.11.007>
- [2] B. Pedrosa, J.A.F.O. Correia, et al. Fatigue resistance curves for single and double shear riveted joints from old Portuguese metallic bridges. *Eng Fail Anal* 2019; 96:255-273. <https://doi.org/10.1016/j.engfailanal.2018.10.009>
- [3] G. Lesiuk, J.A.F.O. Correia, et al. Fatigue crack growth rate of the long term operated puddle Iron from the Eiffel bridge. *Metals* 2019; 9(1), Article No. 53. <https://doi.org/10.3390/met9010053>
- [4] G. Lesiuk. Application of a new, energy-based ΔS^* crack driving force for fatigue crack growth rate description. *Mater* 2019;12(3), Article No. 518. <https://doi.org/10.3390/ma12030518>
- [5] ASTM E407-07(2015)e1 Standard Practice for Microetching Metals and Alloys, ASTM International, West Conshohocken, PA, 2015, <https://doi.org/10.1520/E0407-07R15E01>
- [6] G. Lesiuk, M. Szata, J. A. Correia, A. M. P. De Jesus, F. Berto, (2017). Kinetics of fatigue crack growth and crack closure effect in long term operating steel manufactured at the turn of the 19th and 20th centuries. *Engineering Fracture Mechanics*, 185, 160-174. <https://doi.org/10.1016/j.engfracmech.2017.04.044>
- [7] G. Lesiuk, M. Szata, M. Bocian (2015). The mechanical properties and the microstructural degradation effect in an old low carbon steels after 100-years operating time. *Archives of Civil and Mechanical Engineering*, 15(4), 786-797. <https://doi.org/10.1016/j.acme.2015.06.004>
- [8] G. Lesiuk, J. Correia, M. Smolnicki, A. De Jesus, M. Duda, P. Montenegro, R. Calçada, (2019). *Fatigue Crack Growth Rate of the Long Term Operated Puddle Iron from the Eiffel Bridge*. *Metals*, 9(1), 53. <https://doi.org/10.3390/met9010053>
- [9] ASTM International, 2015. ASTM E647 - 15 Standard Test Method for Measurement of Fatigue Crack Growth Rates. In United States: ASTM International, p. 43. Available at: <http://www.astm.org/Standards/E647>. <https://doi.org/10.1520/jai13180>
- [10] W. Elber 1970, Fatigue crack closure under cyclic tension, *Engineering Fracture Mechanics*, 2, pp. 37-45, 1970. [https://doi.org/10.1016/0013-7944\(70\)90028-7](https://doi.org/10.1016/0013-7944(70)90028-7)
- [11] G. Lesiuk (2019). Mixed mode (I+II, I+III) fatigue crack growth rate description in P355NL1 and 18G2A steel using new energy parameter based on J-integral approach, *Engineering Failure Analysis*, 93, 263-272. <https://doi.org/10.1016/j.engfailanal.2019.02.019>
- [12] G. Lesiuk, M. Szata, D. Rozumek, Z. Marciniak, J. Correia, A. De Jesus, (2018). Energy response of S355 and 41Cr4 steel during fatigue crack growth process. *The Journal of Strain Analysis for Engineering Design*, 53(8), 663-675. <https://doi.org/10.1177/0309324718798234>